MEMOIRS OF GRADUATE SCHOOL OF ENG. *TOKYO METROPOLITAN UNIV.* No. 51, 2001

Microwave Properties of Rock Salt and Limestone for an Ultra-High Energy Neutrino Detector *

Toshio Kamijo †, Masami Chiba*, Miho Kawaki**, Masahide Inuzuka***

Synopsis

Rock salt and limestone are studied to determine their suitability for use as a radio wave transmission medium in an ultra high energy (UHE) cosmic neutrino detector. The detector would detect radio waves generated by the Askar'yan effect (coherent Cherenkov radiation from negative excess charges in an electromagnetic shower) in the interaction of the UHE neutrinos with the high-density medium. We have measured the complex permittivity of the rock salts and limestone by a free space method and a perturbational resonator method in the laboratory at 9.4GHz. We have estimated the microwave attenuation lengths in the samples and find that our estimate of the attenuation length of the rock salt samples from the Asse mine in Germany are longer than 310m at 100 MHz under the consumption of constant tanδ with respect to frequency.

1. Introduction

Several cosmologically distant astrophysical systems, e.g. active galactic nuclei, produce ultra-high-energy (UHE) cosmic neutrinos [1] of energies over 10^{15} eV (PeV) whose flux, though very low, probably exceeds that of atmospheric neutrinos [2]. Therefore, despite the low flux and the low cross section, we can detect extraterrestrial neutrinos coming from distances over 100 Mpc (10 million light years) without an atmospheric neutrino background. On the other hand, in spite of the GZK (Greisen, Zatsepin and Kuz'min) cutoff [3,4], protons of energies over 1020 eV arrive to the earth [5]. Due to this proton flux, we expect a neutrino flux to be produced by process between the high-energy protons and the relic cosmic microwave background of 2.7K or cosmic relic neutrinos of 1.9K.

The aim of UHE-neutrino detection is to study (1) the UHE neutrino interaction, which is not afforded by artificial neutrino beams generated in an accelerator, (2) the neutrino mass problem through the neutrino oscillation effect after a long flight distance [6-8] and (3) the UHE accelerating mechanism of the protons existing in the universe. [interstellar protons].

In order to detect UHE neutrinos, we need a detector with a huge mass (at least 10^9 tons) since neutrinos interact in the detector volume only via weak interactions and the flux of UHE neutrinos is very low [9-11].

---

* Manuscript ID: MGSE2001-2-9 / Received February 20, 2002

† Research Associate, Department of Electrical Engineering
* Research Associate, Department of Physics, Graduate School of Science
** Hitachi Software Engineering Co. Ltd.
*** Department of Physics, Graduate School of Science

However, from a practical point of view, it is difficult to construct such a huge detector. We are therefore interested in the possibility of using a natural rock salt mine as a UHE neutrino detector, a Salt Neutrino Detector (SND) [10]. Rock salt deposits are distributed world wide [12] so there are many candidates for suitable sites. Rock salt deposit does not allow water penetration, which hinders radio wave transmission. Fig.1 is shows a scheme for an SND using a large volume of salt dome (1km x 1km x 1km).

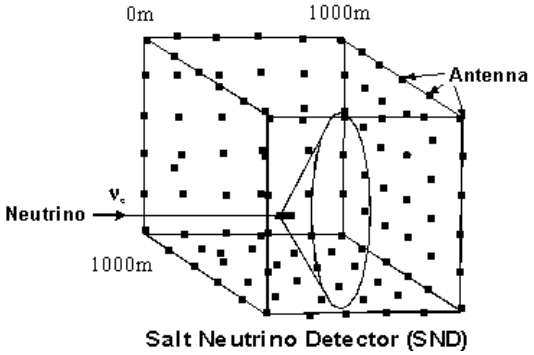

Fig. 1 Underground Salt Neutrino Detector. Excess electrons in the shower from the UHE neutrino interaction generate coherent Cherenkov radiation with an emission angle of 66°.

In order to detect UHE neutrinos, we need a detector with a huge mass (at least 10^9 tons) since neutrinos interact in the detector volume only via weak interactions and the flux of UHE neutrinos is very low [9-11]. However, from a practical point of view, it is difficult to construct such a huge detector. We are therefore interested in the possibility of using a natural rock salt mine as a UHE neutrino detector, a Salt Neutrino Detector (SND) [10]. Rock salt deposits are distributed world wide [12] so there are many candidates for suitable sites. Rock salt deposit does not allow water penetration, which hinders radio wave transmission. Fig.1 is shows a scheme for an SND using a large volume of salt dome (1km x 1km x 1km).

In order to measure UHE neutrinos effectively, the mass of a detector should be considerable greater than that of the existing large neutrino detector, the Super Kamiokande (S-K), Kamioka, Gifu, Japan, which consists of 5×10^4 tons of pure water [13]**.** The S-K detects visible light generated by the Cherenkov Effect in pure water. The transparency (attenuation length) of pure water is 100 m at most.

Rock salt, on the other hand, is one of the most transparent materials for radio waves [14-17] as well as ice. Therefore a moderate number of radio wave sensors could detect neutrino interactions in the massive rock salt. G. A. Askar'yan has proposed detecting radio emissions with coherent amplification produced by excess negative charges of electron-photon showers in dense materials, the Askar'yan Effect [18], which could be used to detect the interaction of UHE neutrinos with high-density media. The radio wave generation mechanisms of an SND have been discussed by several researchers [19-23] and recently the Askar'yan Effect was confirmed by a bunched electron beam in an accelerator [24,25]. The transparency to electromagnetic waves in the microwave region or longer wavelengths is expected to be larger in rock salt than in pure water. Therefore a moderate number of radio wave sensors could detect neutrino interactions in the massive rock salt [12,20].

Unfortunately, no natural rock salt deposits are located in Japan. At the age of rock salt formation, Japan was under the sea, and hence there was no possibility for deposits to form. To find possible locations for constructing an SND we have visited five rock salt mines outside Japan and taken samples of the rock salt.

We have also considered the possibility of using limestone as a detector mass. In Japan limestone mines are abundant and the proportion of $CaCO_3$ in Japanese limestone is over 95%, compared with around 80% in limestone from overseas sources. We have taken samples of limestone from a mine at Kamaishi to examine its viability as a detector.

We have previously reported measurements of the complex permittivities of rock salt samples by a free space method [10]. In the present report we present results of measurements of rock salt and limestone samples by a perturbative cavity resonator method in which the precision of the imaginary part (the attenuation in a medium) of the permittivities is improved.

2. Measurement of complex permittivity using metal-backed sheet samples by the free space measurement method.

To begin with, we restate our results of the space measurement method on rock salt (c.f. Ref. [10]). Three rock salt samples were used for the measurement of the complex permittivity by the free space measurement method. Two were taken from the Hallstadt salt mine in Austria and the third from the Asse salt mine in Germany. Each of the samples was prepared into sheets 200 mm × 200 mm square, as shown in Fig. 2. The samples from the Hallstadt mine were 30 mm and 11 mm thick, and the sample from the Asse mine was 99 mm thick.

(a) 200mm×200mm×30mm (b) 200mm×200mm×11mm (c) 200mm×200mm×99mm

Fig. 2 Photos of rock salt samples from (a), (b) the Hallstadt salt mine, Austria, and (c) the Asse salt mine, Germany. The samples from the Hallstadt salt mine are brown in color and have a striped pattern to their coloration. The sample from the Asse salt mine is white and has no striped pattern. The rock salt appears to consist of small single crystals.

A free space measurement method was employed and is illustrated in Fig. 3. This method has been used in a non-destructive manner for the assessment of microwave absorbers [27-30]. The method involves measuring the amplitude and phase of scattered radiation with and without a metal-plate reflector on the sample. We use a vector network analyzer HP85107A to make the measurements. An important feature of the method is the ability to subtract extraneous scattering from the scattering of interest. The scattering of interest is that of the area where the metal-plate reflector is placed, namely the measuring area. Extraneous scattering is scattering from the walls, ceiling or floor, or from parts of the sample outside the measuring

area as well as non-scattered radiation that passes directly from the transmitting antenna to the receiving antenna. By making measurements of the scattered radiation first with and then without the metal-plate reflector, the incident radiation and the radiation scattered off the measuring area can be separated from the extraneous scattering. The behavior of the metal-plate reflector is similar to that of an optical shutter in optics. A photograph of the equipment with a rock salt sample from the Asse salt mine is shown in Fig. 4.

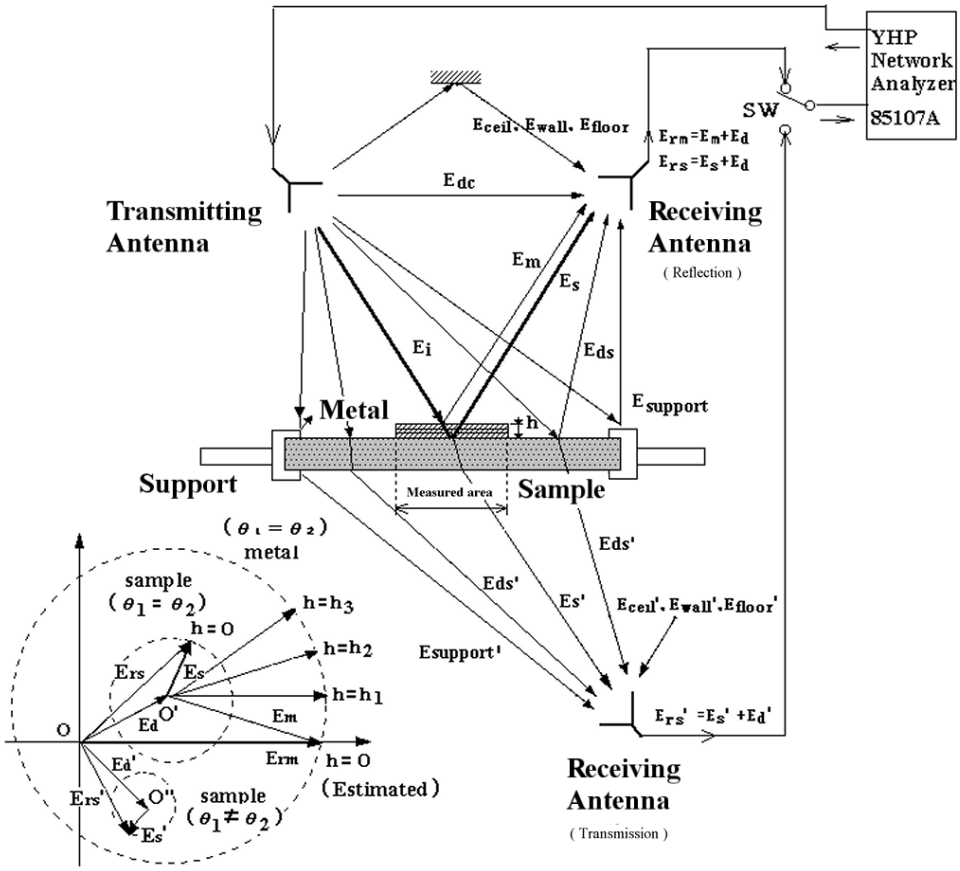

Fig. 3 The principle of the measurement of the free space method showing the various wave components. The signals both with and without the metal-plate reflector on the sample are also shown in a vector diagram. (See text for the definitions of the symbols.)

Fig. 4 Photograph of the measuring apparatus operating in the X-band with a sample from the Asse salt mine. The transmitting and receiving horn antennas are set on a 2.6 m diameter arch above the samples such that both the incident and reflection angles are 5°.

In Fig. 3, the illustration shows three metal plates piled up on the sample to keep the reflector surface elevated. The receiving antenna may be set up for either measuring reflected or transmitted radiation. We consider here the reflective case. $\boldsymbol{E_m}$, $\boldsymbol{E_s}$ and $\boldsymbol{E_d}$ refer to scattered signals from the metal plate, the measuring area of the sample and background objects, respectively. The received signals $\boldsymbol{E_{rm}}$ and $\boldsymbol{E_{rs}}$ are the scattered signals from the metal-plate reflector $\boldsymbol{E_m}$ with the background signal $\boldsymbol{E_d}$, and from the measuring area of the sample $\boldsymbol{E_s}$ with the background signal $\boldsymbol{E_d}$. The height of the metal-plate reflector is raised to give a small difference in the path length between the antennas and the metal-plate reflector, which alters the phase of the scattered wave from the metal-plate reflector only. In the vector diagram, the horizontal and the vertical axes express the real and the imaginary coordinates. The large and small circles show the cases with and without the metal-plate reflector. Different heights of the metal-plate result reflector in different path lengths, expressed as h = 0, h_1, h_2 and h_3 on the large circle and the $\boldsymbol{E_m}$ vectors are shown (note that $\boldsymbol{E_{rm}}$ is illustrated only for the case of h = 0). On the small circle, $\boldsymbol{E_s}$ is shown only at h = 0, without the metal-plate reflector. The center of each of the circles defines $\boldsymbol{E_d}$, and hence it can be deducted and the background eliminated.

As shown in Fig. 4, the sample was lain horizontally on a metal table, which could be raised or lowered to adjust the height of the surface of the metal-plate reflector or the sample. Microwaves were irradiated downward with an incident angle of 5° to the sample by a horn antenna with an aperture of 97 mm × 68 mm at 8.0-10.0 GHz. The reflected radiation was detected by another horn antenna of the same aperture also at 5°. The distance from the horn antennas to the sample was 1.3 m.

Measurements were taken with the sample and the metal-plate reflector at a number of different heights. The real and imaginary components of seven measured signals are plotted in Fig. 5 with (circles) and without (crosses) the metal-plate reflector.

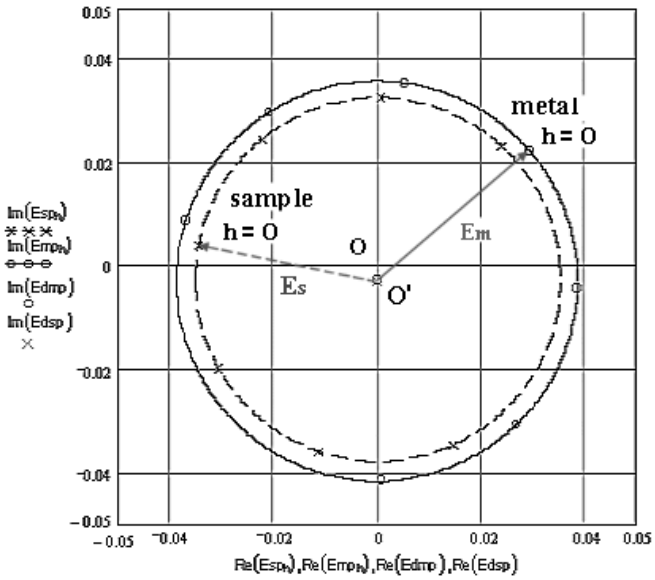

Fig. 5 Seven measurements made at different heights separated by 2 mm. The measured complex values of the received signal are plotted for each position with (circles) and without (crosses) the metal plate. The figure is in parallel polarization with the scattering plane. Circles were drawn through the measured points, a solid line with the reflector and a dashed line without, and the centers were found to be coincident.

Fig. 5 also shows the vectors $\boldsymbol{E_{rm}}$, from the origin to the circumference of the large circle formed by the circles, and $\boldsymbol{E_{rs}}$, to the circumference of the small circle formed by the crosses, in parallel polarization with the scattering plane. The centers of the two circles coincide precisely, hence the background signal $\boldsymbol{E_d}$ is the same in both cases. Also, as the centers are very close to the origin, $\boldsymbol{E_d}$ is small. In the case of a single reflection at the bottom surface of the sample, the differences in angle and radius between $\boldsymbol{E_{rm}}$ and $\boldsymbol{E_{rs}}$ in the complex plane correspond to the real and imaginary permittivities. In practice however, multiple paths between the upper and lower surfaces inside the sample must be accounted for. The complex permittivity can be deduced from the scattering coefficient, the ratio of the complex reflection coefficients, $\boldsymbol{R_{p,s}} = \boldsymbol{E_s}/\boldsymbol{E_m}$, where p and s refer to parallel and perpendicular polarizations with respect to the scattering plane.

We can calculate the attenuation coefficient α for the case of a low loss material from the equation

$$\alpha = \frac{\omega}{c}\sqrt{\varepsilon'}\,\frac{\tan\delta}{2}, \tag{1}$$

where the complex permittivity ε is

$$\varepsilon = \varepsilon' - j\varepsilon'' = \varepsilon'(1 - j\tan\delta), \tag{2}$$

and the loss angle in the permittivity tanδ is

$$\tan\delta = \frac{\varepsilon''}{\varepsilon'}. \tag{3}$$

From $\boldsymbol{\varepsilon}$ and tanδ we can calculate the complex refractive index n,

$$n = \sqrt{\varepsilon} = \sqrt{\varepsilon'}\sqrt{1 - j\tan\delta}. \tag{4}$$

After traveling a distance z through a material, the complex electric field of the electromagnetic wave $\boldsymbol{E_0}$ becomes $\boldsymbol{E}$,

$$E = E_0 e^{j\omega t-(\alpha+j\beta)z} = E_0 e^{-\alpha z} e^{j(\omega t-\beta z)} \tag{5}$$

where the propagation constant $\boldsymbol{\gamma} = \alpha + \boldsymbol{j}\,\beta$ can be expressed as

$$\alpha + j\beta = j\omega\sqrt{\varepsilon_o \mu_0}\,\sqrt{\varepsilon' - j\varepsilon''}. \tag{6}$$

The scalar electric field decreases as

$$|E| = |E_0| e^{-\alpha z} \tag{7}$$

Therefore the electric field attenuation length L_α where the field strength decreases by a factor of 1/e is

$$L_\alpha = \frac{1}{\alpha} \tag{8}$$

The calculated real part of the complex permittivities of the three samples derived from $\boldsymbol{R_p}$ and $\boldsymbol{R_s}$ are tabulated in Table 1. The estimated uncertainty in each of the real values is ± 0.2. The values of the real part are consistent each other and with the value of 5.9 in the reference material [14]. The measurement accuracy was insufficient to allow the imaginary part of the permittivity to be calculated. We found that the imaginary permittivity had different values for samples (a) and (b), even though both were cut from the same block. We were able to estimate that the imaginary part of the permittivity is less than 0.1, or tanδ is less than 0.017 at 9.4 GHz.

TABLE 1. Real part of complex permittivities in rock salts

Sample thickness	Calculated from R_p	Calculated from R_s
(a) Hallstadt 11.1mm	5.9 ± 0.2	6.0 ± 0.2
(b) Hallstadt 30.1mm	5.9 ± 0.2	6.0 ± 0.2
(c) Asse Mine 99.0mm	5.9 ± 0.2	5.9 ± 0.2

Using our estimate for the upper limit of tanδ of 0.017, we calculate a lower limit on α of 4.1 m^{-1} at 9.4 GHz. Hence the attenuation length L_α is greater than 0.24 m at 9.4 GHz. Assuming that tanδ is constant with respect to frequency, the attenuation length is larger than 24 m at 94 MHz.

Unfortunately, the accuracy of this method as used in this experiment is too poor for these low tanδ samples. A more accurate value for tanδ could be achieved if we used a sample with a larger area and thickness and used the transmission configuration. This method also has the advantage in that it can be

modified to make *in situ* measurements. However, in order to improve our results we have chosen to measure the permittivities of rock salt and limestone using the cavity perturbation method.

3. Measurement of complex permittivity using a small stick sample by the cavity perturbation method.

We have measured natural rock salt samples by the perturbed cavity resonator method at 9.4 GHz [31]. The measuring system is shown in Fig. 6. Note that there are no sample insertion holes in the cavity. A drawing and photograph of the rectangular cavity are shown in Fig. 7. The Q value (ratio of resonance frequency to the resonance width) of this system is around 4000. For this perturbation method small samples, such as 1 mm × 1 mm × 10.2 mm, should be used in order to avoid changing the resonance behavior significantly, e.g. inducing only a small shift in the resonance frequency and resonance width. In addition, the electric field strength should be uniform over a cross section of the sample. It is difficult to cut fragile samples to this size. Mechanical cutting using a milling machine was unsatisfactory for our natural rock salt samples. Synthesized rock salt in single crystals could be cleaved to the size, but it was difficult to cleave natural rock salt and slightly thicker samples of natural rock salt had to be used. Limestone is strong enough and we could cut it with a milling machine.

Magnetic field couplings were used for the input and output couplings. The cavity width (in the x-direction) and height (in the y-direction) were set to a = 22.9 mm and b = 10.2 mm, respectively. The cavity length L, however, was adjustable so that filling factor of the sample could be varied. The resonance mode is defined by the parameter $TE_{10n,}$ where the three numbers of the subscript refer to the number of nodes in the x, y and z directions respectively, i.e. there is 1 node in the x direction, 0 in the y direction and n for the z direction can be varied by varying the length of the cavity. With the sample in the center of the cavity, n can be set to 1, 3, 5, 7 or 9, and refers to the number of half guided-wavelengths $\lambda_g/2$ in the wave-guide. Hence n is set by varying the length of the cavity with each half wavelength equal to $\lambda_g/2$ = 22.2 mm.

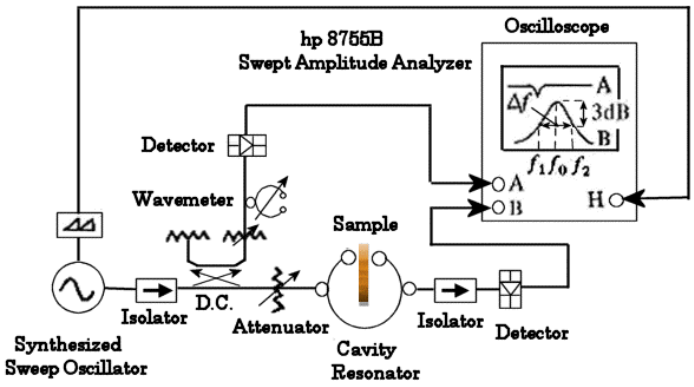

Fig. 6 Drawing of the cavity resonator system.

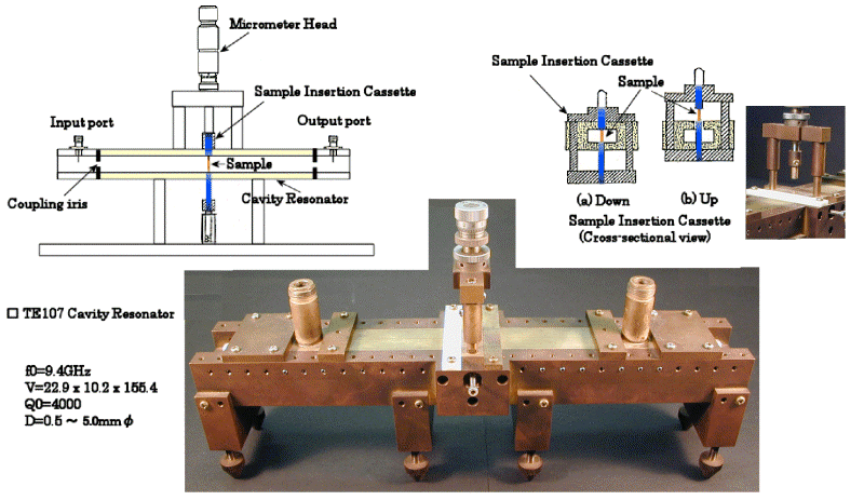

Fig. 7 Illustration and photograph of the perturbed cavity resonator without insertion holes [31].

For these measurements, we take n = 7 to give a sharp resonance in the cavity. This gives a cavity resonator length of L = 155.4 mm. The resonance wavelength λ_0 is calculated by

$$[\frac{1}{\lambda_0}]^2 = [\frac{1}{2a}]^2 + [\frac{n}{2L}]^2. \tag{9}$$

For the values of n, L and a defined above the free space wavelength λ_0 becomes 31.9 mm with a frequency of c/λ_0 = 9.404 GHz.

Using this apparatus the complex permittivity ε could be measured. The principle of the measurement is to derive the real and imaginary parts of the complex permittivity, ε' and ε'', from the changes in the center frequency and the width of the resonance, respectively. Measurements were made both with and without the insertion of the sample in the cavity.

The real ε' is found from the change in resonance frequency when the sample is placed in the cavity,

$$\frac{-(f - f_0)}{f_0} = \alpha_\varepsilon (\varepsilon' - 1)\frac{dV}{V} \tag{10}$$

where f and f_0 are the resonance frequencies with and without the sample in the cavity, dV and V are the volumes of the sample and the cavity resonator, and α_ε is a constant determined by the mode of the cavity and the sample position relative to the electric field maximum—equal to 2 in this case of TE_{107}. Note that the appearance of dV/V indicates that the size of the sample impacts on the perturbation of the resonance behavior and hence a small stick-shaped sample should be used.

The imaginary ε'' depends on the change in the Q factor,

$$\frac{1}{2}[(\frac{1}{Q}) - (\frac{1}{Q_0})] = \alpha_\varepsilon \varepsilon'' \frac{dV}{V} \tag{11}$$

where Q and Q_0 are f/df and f_0/df_0, respectively, and df (~2.7MHz)and df_0 (~2.5MHz) are the resonance widths measured at a height of half the peak height. The inverse Q difference $(1/Q - 1/Q_0)$ is defined as $1/Q_s$. Equations (10) and (11) is called perturbation formula. The measured Q_0 was found to be around 4000. A radio frequency signal was supplied to the cavity resonator by a synthesized CW generator (Anritsu 68047C) and Q was measured by a HP8755B swept amplitude analyzer. The absolute uncertainty of the frequency measurements was well under 1×10^{-5}.

The measurement uncertainty in ε' comes from an uncertainty of ~10 kHz from measuring the resonance peak frequencies and an uncertainty of ~0.001 mm^3 from measuring the volumes of the cavity and the sample. The largest contribution to the uncertainty in determining ε' was from the measurement of dV. The sample volume was measured by a microscope furnished with movable x-y micrometers. We estimate an uncertainty in ε' of 3%.

The uncertainty in ε'' is mainly due to the uncertainty in measuring the resonance width, ~100 kHz, with and without the sample. After the calculation, the estimated uncertainty in ε'' is 2.5×10^{-4}. The variation in the measured values is greater than this uncertainty, even though those samples were cut from the same block. This variation may be due to differences in impurity through the block and hence the ε'' of a sample depends on where the sample is cut from the block. Differences in the smoothness of the surface, the stain and the moisture content may also lead to variations in ε''. In addition, the apparatus itself may lead to variations. Multiple reflections of the radio wave in the input and output wave guides between the cavity and the RF generator and between the cavity and the detector might lead to changes in the output amplitude.

Fig. 8 Samples measured with the perturbative cavity resonator

We were able to cleave four synthetic rock salt samples into single crystals of cross sections ranging from 1.0 mm × 1.1 mm to 1.0 × 1.6 mm with filling factors dV/V of 3.2×10^{-4} to 4.6×10^{-4}. For filling factors this small ε' and ε'' are not affected by perturbations to the resonance due to the presence of the sample. For synthetic rock salt, we found an average $\varepsilon = (5.8 \pm 0.2) - j\ (3.2 \pm 0.3) \times 10^{-3}$ or $\tan\delta = (5.5 \pm 0.5) \times 10^{-4}$, which is consistent with the values given in Ref. [21]. We have succeeded in cleaving samples of natural rock salt from the Asse salt mine in Germany and the Hallstadt salt mine in Austria and have milled samples of limestone from the Kamaishi limestone mine. The samples were formed into small sticks of length 10.2 mm, equal to the height of the cavity resonator. Fig. 8 shows a photograph of these small stick samples and their cross sections are listed in Table 3.

The results of the measurements of ε' and ε'' are listed in Table 2. We find that for the real part of the permittivity ε', the size of the sample is sufficiently thin and the values for the Asse and Hallstadt samples at 5.8 ± 0.2 are consistent with the values for the synthetic rock salt. These values are also consistent with those obtained from the free space measurement, tabulated in Table 1. For the imaginary part of the permittivity ε'', it seems that the samples were not sufficiently thin, in contrast to the synthetic rock salt samples. The results show that the thinner samples have smaller ε'' values. Therefore we are only able to estimate an upper limit for ε'', even for the smallest samples. We have calculated the attenuation coefficient α by Eq. (1). If there is no frequency dependence in $tan\delta$, then since there is no orientational polarization in rock salt and limestone, i.e. ε'' is that same for all orientations, the attenuation lengths L_α, calculated at 9.4 GHz, 7.7 m for the synthetic salt, can be extrapolated to other frequencies e.g. at 94 MHz the attenuation length in a pure rock salt crystal is 770 m. Our results show that at lower frequencies, the attenuation length may be sufficiently long for use in a salt neutrino detector. Although there was a large uncertainty in ε'' we were able to obtain lower limits of the attenuation length.

In order to improve the accuracy of the measurements of ε'' we need thinner samples. Alternatively we could use a super conducting cavity resonator, which would have larger values of Q_0, e.g. 20000. In this case $1/Q_0$ in Eq. (11) becomes smaller and the uncertainty decreases.

If the perturbation formula holds, $-(f-f_0)/f_0$ and $1/Q_s$ are proportional to dV/V. As shown in Fig. 9(a), the linearity of $-(f-f_0)/f_0$ vs. dV/V holds up to a filling factor of about 1.7×10^{-3} for the Asse samples, 2.5×10^{-3} for the Hallstadt samples and 1.1×10^{-3} for the limestone samples. On the other hand, as shown in Fig. 9(b), the linearity of $1/Q_s$ does not hold for any of the samples. Table 3 summarizes the findings of the analysis of the linearity.

TABLE 2. Comparison among single crystal, Asse, Hallstadt rock salt and limestone in ε', ε'', $\tan\delta=\varepsilon''/\varepsilon'$, α at 9.4GHz, $1/\alpha$ at 9.4GHz.

Sample	ε'	$\varepsilon'' \times 10^{-3}$	$\tan\delta \times 10^{-4}$	α at 9.4GHz (m^{-1})	$L_\alpha = 1/\alpha$ at 9.4GHz (m)
Single crystal (NaCl)	5.8 ± 0.2	3.2 ± 0.3	5.5 ± 0.5	0.13 ± .01	7.7±0.7
Asse	5.8 ± 0.2	<78	<13	<0.31	>3.3
Hallstadt	5.8 ± 0.2	<440	<76	<1.79	>0.56
Limestone ($CaCO_3$)	8.3 ± 0.2	<160	<19	<0.54	>1.9

TABLE 3. Comparison among single crystal, Asse, Hallstadt rock salt and limestone in sample cross section, dV/V, linearity of $-(f-f_0)/f_0$ and $1/Q_s = 1/Q-1/Q_0$ in dV/V

Sample	Cross section (mm)	dV/V	Linearity of $-(f-f_0)/f_0$ in dV/V	Linearity of $1/Q_s$ in dV/V
Single crystal (NaCl)	1.0×1.1 – 1.0×1.6	3.2×10^{-4}–4.6×10^{-4}	-	-
Asse	1.7×1.8 – 3.0×3.1	8.5×10^{-4}–2.7×10^{-3}	1.7×10^{-3}	?
Hallstadt	2.1×1.8 – 3.0×3.0	1.0×10^{-3}–2.5×10^{-3}	2.5×10^{-3}	?
Limestone ($CaCO_3$)	1.0×1.0 – 3.0×2.9	2.7×10^{-4}–2.4×10^{-3}	1.1×10^{-3}	?

Fig. 10 measures the dependence of ε' and ε'' on dV/V. In Fig 10(a), ε' is almost constant up to a filling factor of 1.7×10^{-3} for the Asse samples, 2.5×10^{-3} for the Hallstadt samples and 1.1×10^{-3} for the limestone samples. On the other hand, in Fig 10(b), for the Asse samples and limestone ε'' is not constant even at the lowest dV/V.

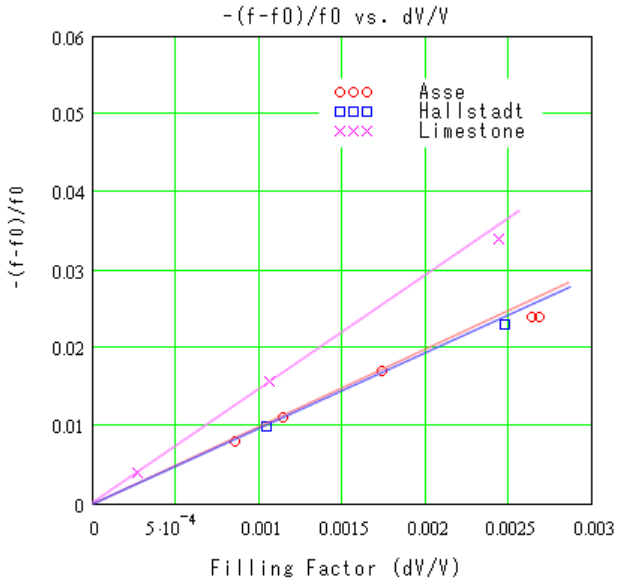

Fig. 9(a) Resonance frequency difference vs. filling factor for rock salt and limestone samples. If the perturbation formula holds, then a straight line should pass through all the data point cross the origin.

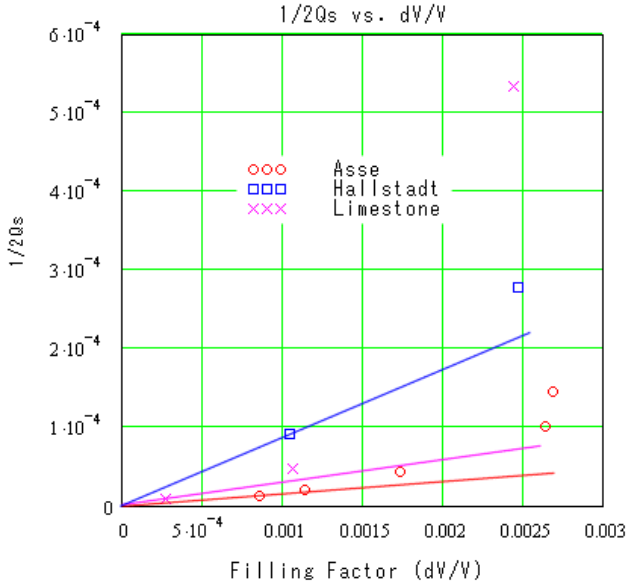

Fig. 9(b) Inverse *Q* difference vs. filling factor for the rock salt and limestone samples. If the perturbation formula holds, then a straight line should pass through all the data points and cross the origin.

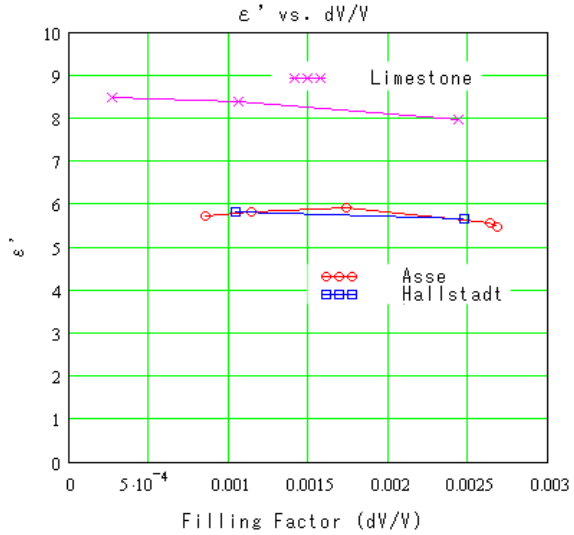

Fig. 10(a) Real part of the permittivity vs. filling factor for the rock salt and limestone samples. If the perturbation formula holds, then all the data points should be constant with respect to the filling factor.

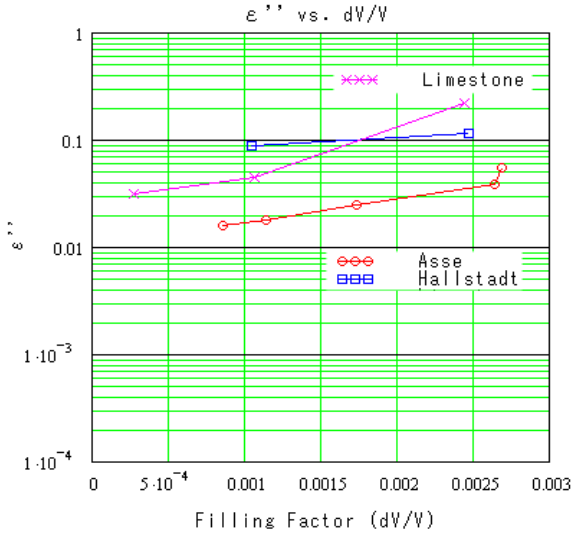

Fig. 10(b) Imaginary part of the permittivity vs. filling factor for the rock salt and limestone samples. If the perturbation approximation holds, all the data points should be constant with respect to the filling factor.

4. Conclusion

Rock salt has been studied as a radio wave transmission medium in a UHE cosmic neutrino detector. The radio waves to be detected are those generated by the Askar'yan effect (coherent Chrenkov radiation from negative excess charges in an electromagnetic shower) for the interaction of UHE neutrinos in the rock salt. Samples from two rock salt mines were investigated to determine whether they are viable sites for an SND. They were the Asse mine in Germany and the Hallstadt mine in Austria. Furthermore, we took limestone samples from a mine in Kamaishi, Japan. We found that they were all potential sites for an SND.

The attenuation lengths of the samples were determined by the free space and cavity perturbation methods. The attenuation lengths of radio wave were found to be 7.7 m, >3.3 m, >0.56 m and >1.9 m at 9.4 GHz for synthetic single crystals, the Asse rock salt, the Hallstadt rock salt and the Kamaishi limestone. A more definite estimate of the attenuation length will require thinner samples. For rock salt the radiation produced by the Askar'yan effect is strongest at about 6 GHz, at the Cherenkov angle of 66°, estimated by the density and the radiation length. At a frequency of 94 MHz the attenuation length is long enough to make a neutrino detector, although the radiation power is compromised and the threshold energy for the detection of neutrinos becomes higher. Recently, P. Gorham et al. [17] have measured attenuation length at the Waste Isolation Pilot Plant (WIPP), located in an evaporite salt bed in Carlsbad, New Mexico and found short attenuation lengths of 3-7m for frequencies of 150-300 MHz. However, measurements at United Salt's Hockley mine, located in a salt dome near Houston, Texas yielded attenuation lengths in excess of 250 m at similar frequencies. Their results are consistent with our result for the Asse sample.

The preliminary results of radio wave attenuation length in rock salt show that it is a possible medium for a UHE neutrino detector in a rock salt mine with a high transparency. However, we need to make perturbed

cavity resonator measurements at lower frequencies and with more samples in order to make a concrete conclusion. Before the SND site is decided it is important to measure the attenuation length *in situ* as there may be defects and impurities in the salt at the site, as well as intrusions by minerals other than rock salt. For such a study a ground penetrating radar would be useful, a well-explored technique.

We have also made a study of a radiometer modified from a television broadcast satellite receiver, which showed a noise level of 150 K, a level low enough for use in an SND. It is a great advantage if we could use low cost receivers such as this as a large number of antennas are required, spaced at less than 200 m in a 1km × 1km × 1km mass of rock salt. The attenuation in the rock salt and the radiation pattern of coherent Cherenkov radiation require that the antennas are repeated in such a way. The frequency to be detected should be decided upon after taking into account the detection energy threshold of the UHE neutrinos and the attenuation length at that frequency. In addition, in order to calibrate the energy of the initial electromagnetic shower produced in the interaction of the neutrinos with the rock salt and the distribution of radiation power, which depends on the degree of coherency, an important study is that of the basic processes of coherent Cherenkov radiation due to a pulsed electron and a neutrino beam in an accelerator [32].

Acknowledgment

This work was supported partly by the Funds for Special Research Project at the Tokyo Metropolitan University, fiscal year 1999. We wish to express our appreciation to Ms. M. Ikeda, Dr. Athar Husain, Dr. O.Yasuda, Prof. K. Minakata and Prof. T. Kikuchi (TMU) for their involvement and support of this project. We express our gratitude to M.E. Ryouichi Ueno who discussed with us and advised us on the microwave techniques. His help was indispensable in carrying out this study.

The research could not be possible without the assistance from and discussions with many people who helped us with the parts of our research which were far from our specialized fields. Here we express our appreciation to those who have taken an interest in our project and provided assistance. The information on and the samples from Austrian rock salt mines were obtained from Prof. Franz Mandl, Prof. Jimmy MacNaughton (Institute for High Energy Physics, Austria), Prof. Komarek (Wien University, Austria), Dr. Doz.Weber (Ministry of Economy, Austria) and Mr. Masayuki Handa (Tobacco and Salt Museum, Tokyo). Prof. Motoyuki Sato (Tohoku Univ.) introduced us to the ground-penetrating radars at the Asse rock salt research mine. We are indebted for our call at the Asse mine and in obtaining the sample to Dr. Dieter Eisenburger (Federal Institute for Geosciences and Natural Resources, BGR, Hanover, Germany), Dr. Stefan Neumaier and Mr. Eberhard Funk (Physikalisch-Technische Bundesansalt, Braunshweig, Germany). Messrs. Nobuteru Hitomi and Yoshiharu Kobayashi (Mechanical Engineering Center, KEK) cut us the rock salt samples.

We appreciate those who informed us about salt domes in petroleum mining: Messrs. Shin-ichi Inoue (Abu Dhabi Oil Co., Ltd.), Hitoshi Takezaki (Japan Energy Development Co., Ltd.), Yoshihisa Tanaka, Taizo Uchimura, Toru Akutsu, Dr. Osamu Takano (Japan National Oil Corporation), and Mr. Greg Jones (Exxon, New Orleans, USA). We are indebted to Prof. Yoshio Nakamura (Institute for Physical Geology, University of Tesax) and Mr. Marcelino Segura (United Salt Corporation, Hockley Plant) for visiting the Hockley Salt Mine (United Salt Co., Houston, Texas, USA). At the visiting to the WIPP, we were taken care of by Prof. Shinjiro Mizutani (Nihon Fukushi Univ.), Dr. Hidekazu Yoshida (Nuclear Fuel Cycle Development Institute), Dr. Erik. K. Webb (Sandia Institute, USA), Dr. Roger Nelson, Ms. Beth Bennington,

and Mr. Norbert T. Rempe (Waste Isolation Pilot Plant, Carlsbad, New Mexico, Department of Energy, USA).

References

1) Stecker, F. W., Done, C., Salamon, M. H., and Sommers, P., "High-Energy Neutrinos from Active Galactic Nuclei", *Phys. Rev. Lett*. **66**, pp.2697-2700 (1991)

2) Barwick, S., Halzen, F., Lowder, D., Miller, T., Morse, Price, P.B. and Westphal, A., "Netrino astronomy on the 1km^2 scale", *J.Phys. G:Nucl. Part. Phys.* **18**, pp.225-247 (1992); Thomas K.Gaisser, Francis Halzen, Todor Stanev, "Particle astrophysics with high energy neutrinos", *Phys. Reports* **258**, pp173-236 **(**1995); Alvarez-Muniz and Halzen F., "1020eV cosmic-ray and particle physics with kilometer-scale neutrino telescopes", Phys. Rev. **D63**, 037302-1, 037302-4 (2001)

3) Greisen, K., "End to the Cosmic-Ray Spectrum?" *Phys. Rev. Lett*. **16**, p.748 (1966); Zatsepin, G.T., Kuz'min, V.A., *Zh. Eksp. Teor. Fiz*., *Pis' ma Red.* **4**, p.114 (1966) [*Soviet Physics JETP Lett.* **4**, p.78 (1966)]

4) Burdman, G., Halzen, F. and Gandhi, R., "The highest energy cosmic rays and new particle physics", *Phys. Lett.* **B417***,* pp.107-113 (1997); Jain, P., Mckay, D.W., Panda, S., Ralston, J. P., "Extra dimensions and strong neutrino-neutrino-nucleon interactions above 10^{19}eV: breaking the GZK barrier", *Phys. Lett.* **B484**, pp.267-274 (2000)

5) Takeda *et al*., "Extension of the Cosmic-Ray Energy Spectrum beyond the Predicted Greisen-Zatsepin-Kuz'min Cutoff", *Phys. Rev. Lett*. **81**, pp.1163-1166 (1998)

6) Athar H, Parente G. and Zas E, "Prospects for observations of high-energy cosmic tau neutrinos", Phys. Rev. D**62**, 093010-1, 093010-5, 2000; Athar H., Jezabek M. and O. Yasuda, "Effects of neutrino mixing on high-energy cosmic neutrino flux"; Athar H., "Effect of neutrino mixing on high-energy cosmic neutrino flux", Presentation at the seminar of high-energy theory group, Oct. 2000, TMU.

7) Halzen, F., Saltzberg, D. "Tau Neutrino Appearance with a 1000 Megaparsec Baseline", *Phys. Rev.Lett***., 81**, pp.4305-4308 (1998)

8) Lerarned, J.G. and Pakvasa, S., *Astropart. Phys*. **3**, 267(1995); Athar, H., Jezabek, M. and Yasuda, O., "Effects of neutrino mixing on high-energy cosmic neutrino flux", *Phys. Rev.* **D62**, 103007-1, 103007-8 (2000); Athar, H., "Tau neutrinos from active galactic nuclei", *Nucl. Phys*.**B (Proc. Suppl.) 76,** 419 (1999); Athar, H., Parente, G. and Zas, E., "Prospects for observations of high-energy cosmic tau neutrinos", Phys. Rev. D62, 093010-1, 093010-5, 2000.

9) Gandhi, R., Quigg, C., Reno, M.H. and Sarcevic I., "Ultrahigh-energy neutrino interactions", *Astroparticle Phys.* **5**, pp.81-110 (1996); "Netrino interactions at ultrahigh energies", *Phys. Rev*.**D58**, 093009: Sigl, G. *Phys. Rev.* **D57**, pp.3786-3789 (1998): Kwiecinski, J., Martin, A.D., Stasto, A.M., "Penetration of the Earth by ultrahigh energy neutrinos predicted by low x QCD", *Phys. Rev***.D59**, 093002 (1999); Horvat, R., "Propagation of ultrahigh-energy neutrinos through the earth", *Phys. Lett*. **B480**, pp.135-139 (2000)

10) Chiba, M., Kamijo, T, Kawaki, M, Athar, H, Inuzuka, M, Ikeda, M., Yasuda, O., "Study of Salt Neutrino Detector", Proc. 1st International Workshop for Radio Detection of High Energy Particles [RADHEP-2000], UCLA (November 16-18, 2000), pp.204-221, AIP Conference Proceedings, Vol. **579**

11) The most recent status of large high-energy neutrino detectors are shown in the presentation transparencies from the 19th International Conference on Neutrino Physics and Astrophysics (Neutrino 2000), 2000, Sudbury, Canada at the URL http://ALUMNI.LAURENTIAN.CA/www/physics/nu2000/.

12) Stanley J. L., "Handbook of World Salt Resources", Plenum Press, New York (1969); Michel T. H., "Salt Domes", Gulf Publishing Company, Houston (1979).
13) Fukuda Y. *et al*., SuperK Collaboration, "Evidence for Oscillation of Atmospheric Neutrinos", *Phys. Rev. Lett*. **81**, 1562(1998).
14) National Astronomical Observatory of Japan (ed.), "Chronological Scientific tables" (in Japanese), Maruzen Co. Ltd., Tokyo, p.486 (1998)
15) Cook, J.C., "Radar Transparencies of Mine and Tunnel Rocks", *Geophysics*, **40**, pp.865-885 (1975)
16) Mundry, E., Thierbach, R., Sender, F and Weichart, H., "Borehole Radar Probing in Salt Deposits", *Proceedings of the Sixth International Symposium on Salt*, **Vol.I**, 585-599 (1983); Nickel, H., Sender, F., Thierbach, R. and Weichart, H., "Exploring the Interior of Salt Domes from Boreholes", *Geophysical Prospecting* **31**, 131-148 (1983); Sato, M. and Thierbach, R., "Analysis of a Borehole Radar in Cross-Hole Mode", *IEEE Transactions on Geoscience and Remote Sensing*, **29**, 899-904 (1991); Eisenburger, D., "Evaluation and Three-Dimensional Representation of Ground-Probing Radar Measurements", *Proceedings of the 5th International Conference on Ground Penetrating Radar*, 647-659 (1994); Eisenburger, D., Gundelach, V., Sender, F., Thierbach, R., "Underground Radar Studies for Solving Geological and Safeguarding Problems in Nuclear Waste Repositories", *Proceedings of the 6th International Conference on Ground Penetrating Radar*, 427-432 (1996).
17) Gorham, P. Saltzberg, D, Odian, A. Williams, D. Besson, D, Fichter, G and Tantawi, S., "Measurements of the Suitability of Large Rock Salt Formations for Radio Detection of High Energy Neutrinos", hep-ex/0108027 v1, 14 Aug 2001.
18) Askar'yan, G.A., "Excess Negative Charge of an Electron-Photon Shower and its Coherent Radio Emission", *Zh. Eksp. Teor. Fiz*. **41**, pp.616-618 (1961) [*Soviet Physics JETP* **14**, pp.441-442 (1962)]; Askar'yan, G.A., "Coherent Radio Emission from Cosmic Showers in Air and in Dense Media", *Soviet Physics JETP* **48**, pp.988 - 990 (1965) [**21**, pp.658 - 659 (1965)].
19) Fujii, M and Nishimura, J. Proc. 11th Int. Conf. On Cosmic Rays, (Butapest, 1969) pp.709-715.
20) Landau, L. D., Pomeranchuk, I. Ya., *Dokl. Akad. Nauk SSSR* **92**, 535 (1953); **92**, 735 (1953); Migdal, A.B., "Bremsstrahlung and Pair Production in Condensed Media at High Energies", *Phys. Rev.*, **103**, 1811-1820 (1956); Klein, S., "Suppression of bremsstrahlung and pair production due to environmental factors", *Rev. Mod. Phys.* **71**, 1501-1538 (1999).
21) Ter-Mikaelian, M. L., "High-Energy Electromagnetic Processes in Condensed Media", Interscience Tracts in Physics and Astronomy, Number 29, Wiley-Interscience, a Division of John Wiley & Sons, Inc., New York (1972), ISBN 0-471-85190-6.
22) Markov, M.A. and Zheleznykh, IM, "Large-Scale Cherenkov Detectors in Ocean, Atmosphere and Ice", *Nucl. Instrum. Methods.* **A248**, pp.242-251 (1986)
23) .Halzen, F., Zas, E.,.Stanev, T, "Radiodetection of cosmic neutrinos. A numerical, real time analysis", *Phys. Lett.* **B257,** 432-436 (1991); Zas, E., Halzen, F., Stanev, T., "Electromagnetic pulses from from high-energy showers: Implications for neutrino detection", *Phys. Rev.* **D45,** 362-376 (1992); Alvarez-Muniz, J. and Zas, E., "Cherenkov radio pulses from EeV neutrino interactions: the LPM effect", *Phys. Lett.***B411,** 218-224 (1997); Frichter, G.M., Ralston, J.P. and .Mckay, D.W., "On radio detection of ultrahigh energy neutrinos in Antarctic ice", *Phys. Rev*.**D53,** 1684-1698 (1996).
24) Gorham, P., Saltzberg, D., Schoessow, Gai, P.W.,.Power, J. G., Konecny, Richard and Conde, M.E., "Radio-frequency Measurements of Coherent Transition and Cherenkov Radiation: Implication for High-energy Neutrino Detection ", *Phys. Rev*. **E62**, pp.8590-8605 (2000)
25) Saltzberg,D., Gorham, P., Walz, D., et al., "Observation of the Askaryan Effect: Coherent Microwave

Cherenkov Emission from Charge Asymmetry in High-Energy Particle Cascades", Phys. Rev. Lett. **86**, p.2802, (2001)
26) Machida, T., *et al*. (ed.), "Topography dictionary" (in Japanese), Ninomiya Book Co. Ltd., Tokyo, p.110 (1981)
27) Ueno, R., Kamijo, T., Hatakeyama, K. and Ogasawara, N., "The Measurement of Scattering Coefficients of Radio-Wave Scatter-Suppressors at the Microwave Region"(in Japanese), Record of Study, I.E.C.E., Japan, CPM 77-106, pp.99-102(1978)
28) Ueno, R. and Ogasawara, N., "On the Measurement of Scattering Coefficient of Radio-Wave Scatter Suppressor", *Memoirs of Faculty of Technology, Tokyo Metropolitan University*, No.30 1980, pp.2907-2916 (1981).
29) Ueno, R. and Kamijo, T., "A Method for the Measurement of Scattering Coefficients at the Microwave Region", *Memoirs of Faculty of Tech., Tokyo Metropolitan University*, pp.3923-3933 (1989)
30) Ueno, R. and Kamijo, T., "Method for the Measurement of Scattering Coefficients Using a Metal-Plate Reflector in the Microwave Region", *IEICE Trans. Commun*. **E83B**, pp.1554-1562 (2000)
31) Ueno, R. and Kamijo, T., "The Measurement of Complex Permittivity Using a Simply Designed Perturbed Cavity Resonator at Microwave Frequencies", *Memoirs of Faculty of Technology, Tokyo Metropolitan University*, No.38 1988, pp.3923-3933 (1989)
32) Camilleri, L. "Neutrino physics at LHC", Large Hadron Collider Workshop, held at Aachen, 4-9 October 1990, Proceedings Vol.III, Editors: G.Jalskog and D.Rein, CERN 90-10 ECFA 90-133 Volume III 3 December 1990.